SHORT COMMUNICATION

Plant Signaling & Behavior 11:2, e1071751; February 2016; © 2016 Taylor & Francis Group, LLC

Phosphorylation at serine 52 and 635 does not alter the transport properties of glucosinolate transporter AtGTR1

Morten Egevang Jørgensen[1,2], Carl Erik Olsen[2], Barbara Ann Halkier[1,2], and Hussam Hassan Nour-Eldin[1,2,*]

[1]Center for Dynamic Molecular Interactions (DynaMo); University of Copenhagen; Frederiksberg, Denmark; [2]Department of Plant and Environmental Sciences; Faculty of Science; University of Copenhagen; Frederiksberg, Denmark

Keywords: glucosinolate transport, membrane transport, NPF2.10 and NPF2.11, POTs, phosphorylation mimicking and *transporter regulation*, secondary active transport, transport phosphorylation, *Xenopus laevis*

Little is known about how plants regulate transporters of defense compounds. In *A. thaliana*, glucosinolates are transported between tissues by NPF2.10 (AtGTR1) and NPF2.11 (AtGTR2). Mining of the PhosPhat4.0 database showed two cytosol exposed phosphorylation sites for AtGTR1 and one membrane-buried phosphorylation site for AtGTR2. In this study, we investigate whether mutation of the two potential regulatory sites of AtGTR1 affected transport of glucosinolates in *Xenopus* oocytes. Characterization of AtGTR1 phosphorylation mutants showed that phosphorylation of AtGTR1 - at the two reported phosphorylation sites - is not directly involved in regulating AtGTR1 transport activity. We hypothesize a role for AtGTR1-phosphorylation in regulating protein-protein interactions.

Plants produce defense compounds to protect themselves against herbivores and pathogens. As defense compounds are metabolically costly to produce,[1] plants have developed strategies to regulate how these compounds are reallocated upon changes in fitness value of a given tissue.[2] From primary metabolites we know that numerous transport proteins are regulated by reversible phosphorylation, including interaction between substructures in the aquaporin SoPIP2;1,[3] activation of the H^+-ATPase AHA2 through protein-protein interaction with a 14-3-3 protein,[4] activation of ion channels,[5-9] activation of PIN-FORMED proteins,[10] and subcellular localization of the aquaporin AtPIP2;1.[11,12] Phosphorylation has also been shown to alter transport kinetics of the IAA/nitrate transporter AtNPF6.3/NRT1.1.[13] In consequence, it is conceivable that phosphorylation could play a role in determining the transport-activity of defense compound transporters. Within the last decade several alkaloid transporters in *Nicotiana* species.[14-16] and *Coptis japonicus*,[17,18] as well as 2 transporters of glucosinolates - a major class of defense compounds in *Arabidopsis thaliana* – were identified.[19,20] The glucosinolate transporters AtGTR1 and AtGTR2 (Arabidopsis Thaliana Glucosinolate Transporter1 and −2, now NPF2.10 and NPF2.11) belong to the NPF (former NRT/PTR) family.[21] NPF2.10/AtGTR1 (AtGTR1) and NPF2.11/AtGTR2/NRT1.10 (AtGTR2) are plasma membrane-localized, high-affinity H^+/glucosinolate symporters, which are essential for the accumulation of glucosinolates in seeds.[20] Grafting experiments that combine *atgtr1 atgtr2* rootstocks with wild-type scions have shown that in the absence of AtGTR1 and AtGTR2 in the root, aliphatic glucosinolates were depleted from roots and over-accumulated in the rosette of 3-week-old plants.[22] This suggests that posttranslational inhibition of AtGTR1 and AtGTR2 transport activity could be a strategy for regulating translocation of aliphatic glucosinolates between organs. In this study, we identify *bona fide in planta* phosphorylation sites in ATGTR1 and AtGTR2, analyze the phosphorylation sites *in silico* and investigate their effect on transport by mimicking phosphorylation at 2 sites in AtGTR1.

To investigate if AtGTR1 and AtGTR2 are phosphorylated *in planta* we searched *The Arabidopsis Protein Phosphorylation Site Database* (PhosPhat4.0).[23] Two phosphorylation sites with a mascot score above 20 were identified for AtGTR1 and one for AtGTR2. AtGTR1 is phosphorylated at Serine 52 and Serine 635.[24-27] The dynamic nature of AtGTR1 phosphorylation was addressed by quantification of phosphopeptides before and after induction with pathogen elicitors.[24,26] Two out of 3 biological repeats showed an up-regulation of phosphorylated AtGTR1-Ser52 upon flg22 elicitor treatment.[26] In another study, where flg22 was used at a different concentration, no dynamic phosphorylation of AtGTR1 was detected.[24] AtGTR2 was reported to be phosphorylated at AtGTR2-Thr58, but no publications are associated.[23]

We analyzed the position of these phosphorylation sites using IMembrane prediction of membrane insertion.[28,29]

*Correspondence to: Hussam Hassan Nour-Eldin; Email: huha@plen.ku.dk
Submitted: 05/28/2015; Revised: 07/07/2015; Accepted: 07/08/2015
http://dx.doi.org/10.1080/15592324.2015.1071751

IMembrane predicts AtGTR2-Thr58 to be situated in the center of the first transmembrane-helix. Furthermore, this site is found in the highly conserved EXXE[R/K] motif and shown to be buried in the membrane segment of the close homolog NRT1.1 where it is facing the substrate tunnel and unlikely to be accessible for kinases.[30] This was confirmed by a SWISS-MODEL generated AtGTR2 homology-model where residue Thr58 is situated in the middle of helix 1 (data not shown). IMembrane predicted AtGTR1-S52 and AtGTR1-S635 to be situated in the non-membrane segment of the protein (**Fig. 1A**). Based on this *in silico* analysis we investigated the effect on transport activity when mimicking phosphorylation and dephosphorylation of AtGTR1-S52 and AtGTR1-S635.

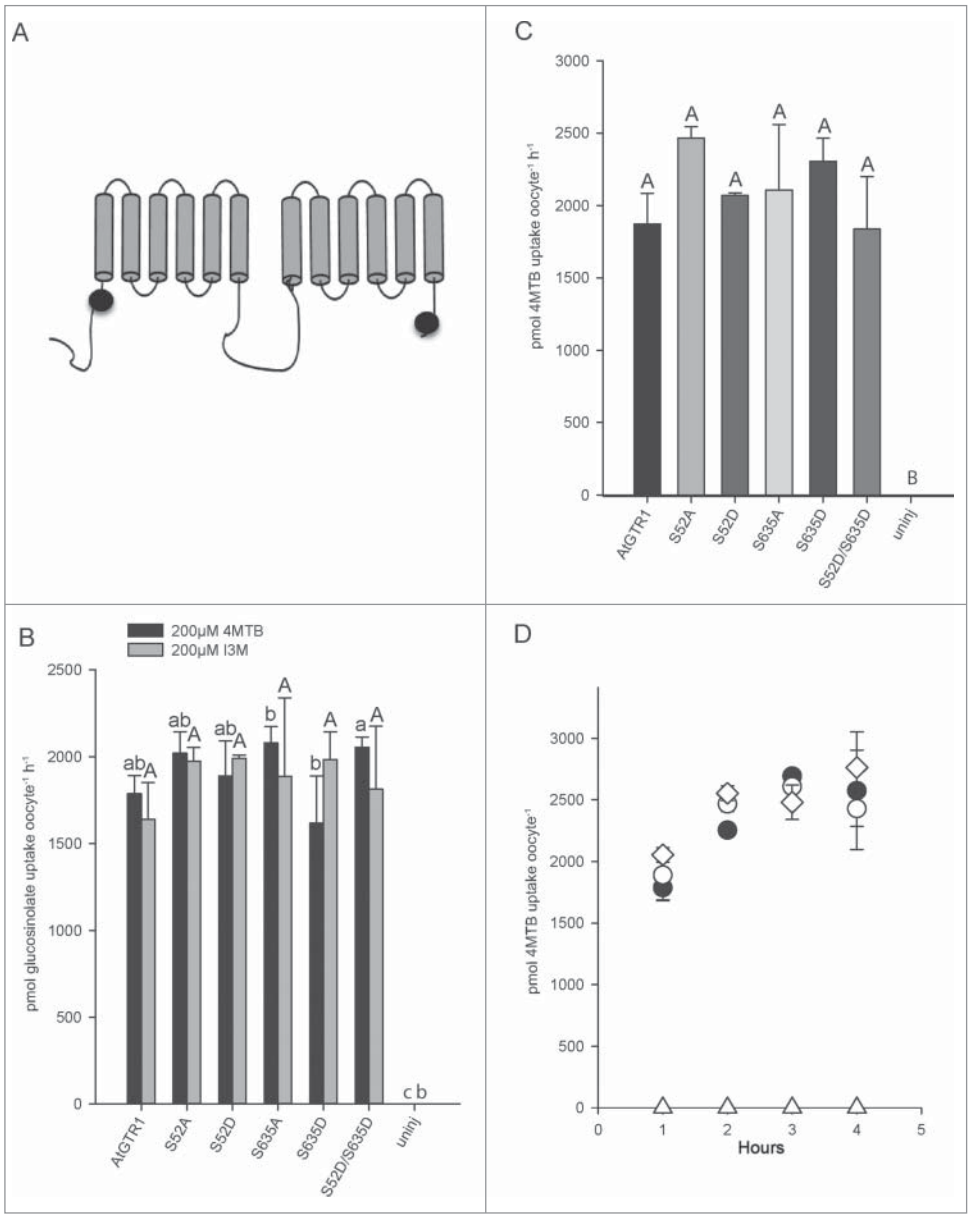

Figure 1. Uptake of 4MTB and I3M by AtGTR1 single and double phosphorylation mimics. **(A)** Predicted 2D membrane topology based on IMembrane predicted membrane insertion highlighting AtGTR1-S52 and AtGTR1-S635 phosphorylation sites reported in Phosphat4.0. **(B-D)** YFP-tagged AtGTR1, S52A, S52D, S635A, S635D and S635D/S52D expressed in *X. laevis* oocytes and characterized for glucosinolate uptake at pH5. **(B)** Glucosinolate uptake activity measured for each AtGTR1 version in the presence of 200μM I3M or 200μM 4MTB for one hour. **(C)** Uptake of 4MTB at saturating concentrations (2000μM) by each of the 6 AtGTR1 versions 1 hour. **(D)** Time course (1-4 hours) of 4MTB uptake at saturating concentrations by S52D and S52D/S635D AtGTR1 versions. Glucosinolate uptake was quantified by LC-MS of oocyte extracts from 3×5 oocytes for each gene. Groups are determined by one-way ANOVA ($P < 0.05$) (Error Bars: SD, n=3).

To investigate how phosphorylation affects the transporters activity we expressed phosphorylation mutants in *X. laevis* oocytes and analyzed aliphatic- (4MTB) and indole-glucosinolate (I3M) uptake by LCMS (**Fig. 1B-D**). In the mutant versions, the serine residues were replaced by either an alanine to mimic a constitutively dephosphorylated state or with aspartic acid to mimic a constitutively phosphorylated state. In total, 5 mutated versions of AtGTR1 were made. These include the single mutants, AtGTR1-S52A, AtGTR1-S52D, AtGTR1-S635A and AtGTR1-S635D and the double mutant AtGTR1-S52D/S635D. We tested the ability of (de)phosphorylation mutants to accumulate substrate when exposed to saturating concentrations of glucosinolates.[20] In addition, we also exposed expressing oocytes to more than 10 times the saturating glucosinolate concentration to investigate if the accumulation capacity was changed for the mutants. No statistically significant difference in glucosinolate accumulation was seen, as calculated by one-way ANOVA ($p < 0.05$), between any of the phosphorylation mutants and wild type AtGTR1 when exposed to 200μM 4MTB or I3M (**Fig. 1B**) and 2000μM 4MTB (**Fig. 1C**). Similar results were obtained when assay time was prolonged to between one and 4 hours (**Fig. 1D**). A small, but significant, difference in accumulation was seen for oocytes expressing S635A and S635D. However, glucosinolate

accumulation by S635D was not significantly different from wild type AtGTR1.

To test if the AtGTR1 mutants had a changed affinity, we measured the apparent K_m values for all mutants (**Fig. 2**). The experiment was made on 2 different batches of oocytes. In the first batch, we measured apparent K_m values for the S52A and S52D mutants in relation to the wild type AtGTR1 version. In the second batch, we measured apparent K_m values for the S635A and S635D mutants in relation to the wild type version.

The S52D mutant appears to display a lowered K_m value, however compared to the already low K_m value for the wild type version (22.7 μM) the value was only reduced by 6 μM, whereas the $K_m$value for the S52A mutant was not different from the wild type version. Similarly the mutants of the S635 phosphorylation site were not different from the wildtype version indicating that the affinity of the transporter is not affected by phosphorylation at these respective sites.

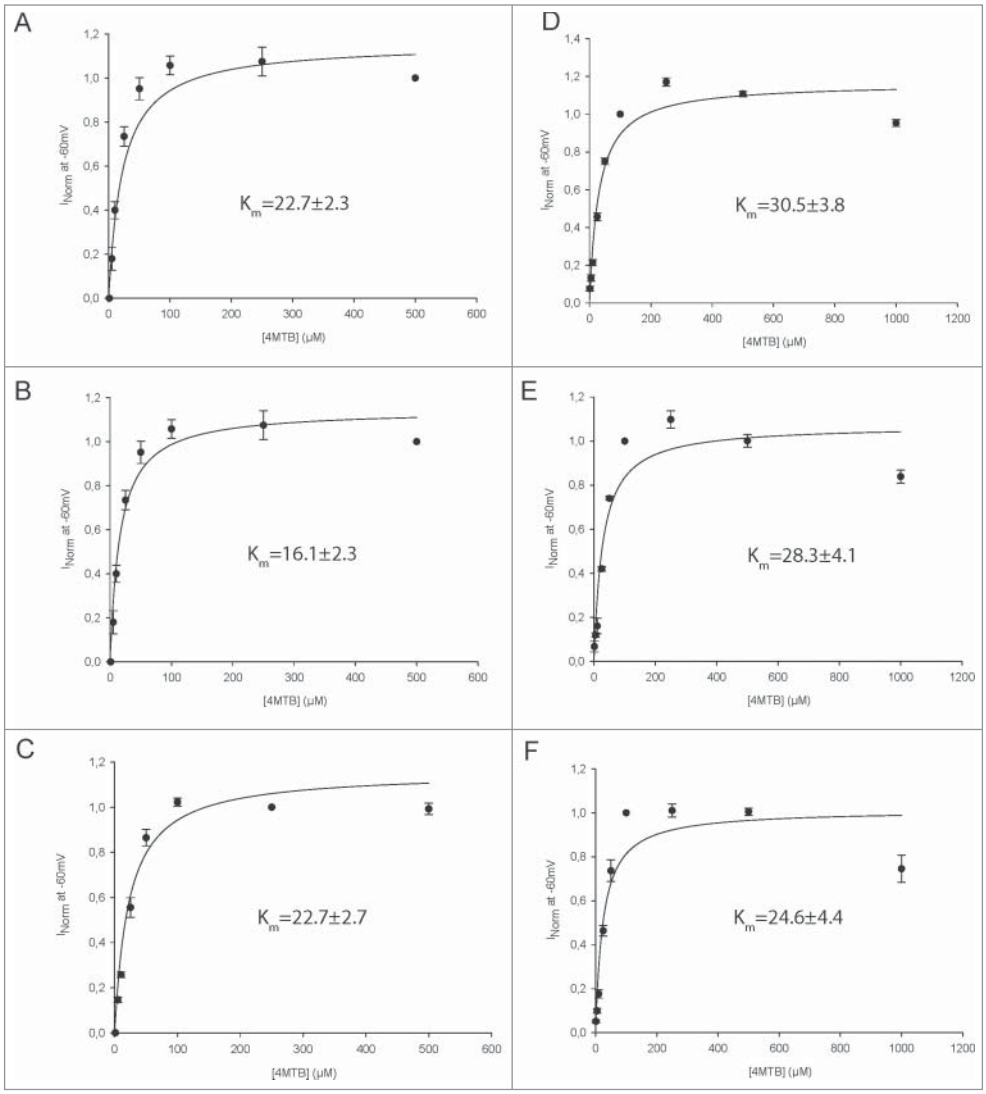

Figure 2. Kinetic analysis of AtGTR1 mutants. **(A-F)** Normalized 4MTB-dependent currents measured at a membrane potential of −60mV and pH5 were plotted against increasing 4MTB concentrations. The saturation curve was fitted with a Michaelis-Menten equation (solid line, error bars are SE, n=4-6 oocytes). Each oocyte dataset was normalized to currents elicited at saturating 4MTB concentration. Apparent K_m measurement for **(A)** S52A,**(B)** S52D, **(C)** Wild type AtGTR1 (control for S52A and S52D, **(D)** S635**(A, E)** S635D, **(F)** Wild type AtGTR1 (control for S635A and S635D) expressing *X. laevis* oocytes.

In this study the regulatory effects of phosphorylation of 2 glucosinolates transporters was investigated. Importantly, rather than predicting phosphorylation sites, the phosphorylation sites were identified by searching the PhosPhat4.0 database,[23] which contains a list of all phosphorylated peptides isolated in phosphoproteomic studies. This increases the likelihood that identified phosphorylation sites have a physiological role *in planta*. Both phosphorylation sites in AtGTR1 were found in studies where plant cell cultures are induced with either stress hormones or bacterial elicitors indicating that the identified phosphorylation sites are important in the plants response to pathogen attack.[24-27]

As we used publicly available data obtained by large scale experiments we analyzed the position of the identified phosphorylation sites *in silico*. As a prerequisite for likely physiological relevance and further experimental analyses we set that a phosphorylation site should be accessible for cytosolic kinases. This means that a phosphorylation site should be exposed to the cytosolic environment and not embedded in transmembrane helices. Predictions of where the first transmembrane helix starts using only sequence based methods such as TMHMM are notoriously imprecise.[31] As a consequence, we used IMembrane which uses homology-based membrane-insertion of proteins to predict the transmembrane helixes more accurately. We combined IMembrane results with SWISS-MODEL generated homology-models to predict whether especially the N-terminally located phosphorylation sites in AtGTR1 and AtGTR2 are free to interact with a kinase in the cytosolic milieu. From our results it was clear that the AtGTR2-T58 residue was buried several α-helix

turns into the membrane. It is therefore unlikely that the phosphorylated peptide deposited in the PhosPhat4.0 database is of AtGTR2 origin. In comparison, both phosphorylation sites in AtGTR1 are located outside transmembrane spanning domains and in segments facing the cytosol. AtGTR1-S52 and AtGTR1-S635 thus appear as *bona fide* phosphorylation sites with potential regulatory functions on transport activity.

We did not measure a reduction in actual glucosinolate uptake activity for oocytes expressing AtGTR1 phosphorylation mutants when assayed over a timespan of an hour or longer. No combinatorial effect was observed when constructing the double phosphorylation mimic AtGTR1-S52D/S635D indicating that these 2 phosphorylation sites do not work in concert to regulate the activity of AtGTR1. We did not measure large differences in apparent affinity toward 4MTB for all single mutants.

Phosphorylation was reported to influence the interaction between a 14-3-3 protein and the proton ATPase AHA2[4] and the interaction between TPK1 and a 14-3-3 protein.[32,33] As phosphorylation mimicking did not affect glucosinolate transport activity as measured by LCMS assays we hypothesize that phosphorylation of AtGTR1 at position S52 and S635 *in planta* recruits another protein important in regulating transport activity by protein-protein interactions.

Primer list

Primer	Name	Sequence
	AtGTR1-S52A non-phosphorylatable mimic	
1	AtGTR1 FW1	GGCTTAAUATGAAGAGCAGAGTCATT
2	S52 FW (S –>A)	ATGTGGTCGAUGCTTTCGAGGAAGAGCAG
3	S52 RV_1 (S–>A/D)	ATCGACCACAUCGGTGTTAGTCGTCGTAGTAG
4	AtGTR1 no stop RV2	GGTTTAAUCCGACAGAGTTCTTGTC
	AtGTR1-S52D phosphorylation mimic	
5	AtGTR1 FW1	GGCTTAAUATGAAGAGCAGAGTCATT
6	S52 FW (S –>D)	ATGTGGTCGAUGATTTCGAGGAAGAGCAG
7	S52 RV_1 (S–>A/D)	ATCGACCACAUCGGTGTTAGTCGTCGTAGTAG
8	AtGTR1 no stop RV2	GGTTTAAUCCGACAGAGTTCTTGTC
	AtGTR1-S635A non-phosphorylatable mimic	
9	AtGTR1 FW	GGCTTAAUATGAAGAGCAGAGTCATT
12	AtGTR1 (S–>A) no stop RV	GGTTTAAUCCGACAGCGTTCTTGTC
	AtGTR1-S635D phosphorylation mimic	
13	AtGTR1 FW	GGCTTAAUATGAAGAGCAGAGTCATT
16	AtGTR1 (S–>D) no stop RV	GGTTTAAUCCGACATCGTTCTTGTC

Materials and Methods

Prediction of membrane insertion

AtGTR1 and AtGTR2 sequences where submitted to the IMembrane server (http://opig.stats.ox.ac.uk/webapps/medeller/home.pl?app=iMembrane) and analyzed.[29]

Homology modeling

AtGTR1 and AtGTR2 sequences where submitted to the SWISS-MODELS server and highest scoring templates was used to generate homology models (http://swissmodel.expasy.org/). AtGTR1 was modeled on the NRT1.1 (NPF6.3) structure (PDB: 4CL4).[34] AtGTR2 was modeled on the NRT1.1 structure (PDB: 4OH3).[30] PDBsum was used to calculate Ramachandran Plot statistics where the AtGTR1 model had 0.8% and AtGTR2 had 1% of residues in disallowed regions, respectively.[35]

Site directed mutagenesis of AtGTR1

Site directed mutagenesis of AtGTR1 to generate AtGTR1-S52A, AtGTR1-S52D, AtGTR1-S635A, AtGTR1-S635D and AtGTR1-S52D/S635D was performed using USER™ Fusion.[36,37] Wild type and mutated coding sequences were cloned into an oocyte expression vector harbouring a C-terminal YFP fluorophore by an advanced uracil-excision-based cloning technique described before.[37]

Heterologous expression of AtGTR WT and mutants in *Xenopus laevis*

Heterologous protein expression in *X. laevis* oocytes was used to characterize WT and point mutated transporters. *In vitro* transcription of cRNA was carried out as described before.[20] Defolliculated *X. laevis* oocytes (states V-VI) were purchased from Ecocyte Biosciences. Injection of 50nl cRNA (500 ng/μl) into *X. laevis* oocytes was done using a Drummond NANOJECT II (Drummond scientific company). Oocytes were incubated for 3 days at 17°C in Kulori pH 7.4, which was changed daily.

Glucosinolate uptake/export assays

4-methylsulfinylbutyl glucosinolate (4MTB) and indol-3-ylmethyl glucosinolate was obtained from C_2 Bioengineering (http://www.glucosinolates.com/) and CFM Oskar Tropitzsch GmbH, Marktredwitz (http://www.cfmot.de/). *X. laevis* uptake assays where carried out as described before.[20]

Electrophysiological measurements and data analysis

All measurements were performed with a Two Electrode Voltage-Clamp system (TEVC) composed of an NPI TEC-03X amplifier (NPI electronic GmbH, Germany) connected to a PC with pCLAMP10 software (Molecular devices, USA) via an Axon Digidata 1440a digitizer (Molecular devices, USA).

TEVC recordings were performed as follows: I) An oocyte was placed in the recording chamber and

perfused with a standard kulori-based solution (90 mM Na-Gluconate, 1 mM K-Gluconate, 1 mM Ca-Gluconate$_2$, 1 mM Mg-Gluconate$_2$, 1 mM $LaCl_3$ and 10 mM MES pH 5). II) The oocyte was impaled by current and potential electrodes in a 45° angel and allowed to heal and equilibrate until the membrane potential was stable. IV) The amplifier was switched to voltage clamp at −60 mV and the oocyte was allowed to establish a stable baseline and currents in the absence of glucosinolate substrate was measured in the voltage range between −30 to −170 mV in 10 mV decrements. V) When the baseline was stable, a standard Kulori based solution with glucosinolate substrate was perfused over the oocyte and currents were recorded in the voltage range between −30 to −170 mV in 10 mV decrements. TEVC data was extracted from pCLAMP10 software as a Microsoft Excel compatible worksheet and analyzed in Excel. Glucosinolate induced currents was calculated by subtracting currents before addition of glucosinolate substrate from currents after addition of glucosinolate substrate. SigmaPlot version 12.3 (Systat software, USA) was used for statistical analysis and data plotting. Visualization and curve fitting to the Michaelis-Menten equation (**Equation 1**) to calculate the apparent K_m value was done using SigmaPlot version 12.3 (Systat software, USA).

Equation 1-Michaelis-Menten equation. I is the current, I_{max} is the maximal current achieved by the transporter at saturating concentrations of 4MTB

$$I = \frac{I_{max} * [4MTB]}{[4MTB] + Km} \quad (1)$$

Desulfo glucosinolate analysis of X. laevis oocytes by LC-MS or HPLC

ESI-LC-MS analysis of desulfo glucosinolates from *X. laevis* uptake assays was performed as described before.[20]

Statistical Analysis

SigmaPlot version 12.3 (Systat software, USA) was used for statistical analysis (one-way ANOVA and the TUKEY test) and data plotting.

Disclosure of Potential Conflicts of Interest

No potential conflicts of interest were disclosed.

References

1. Züst T, Heichinger C, Grossniklaus U, Harrington R, Kliebenstein DJ, Turnbull LA. Natural Enemies Drive Geographic Variation in Plant Defenses. Science 2012; 338:116-9; PMID:23042895; http://dx.doi.org/10.1126/science.1226397
2. Jørgensen ME, Nour-Eldin HH, Halkier BA. Transport of defense compounds from source to sink: lessons learned from glucosinolates. Trends Plant Sci 2015; 8:508-514; PMID:25979806
3. Tornroth-Horsefield S, Wang Y, Hedfalk K, Johanson U, Karlsson M, Tajkhorshid E, Neutze R, Kjellbom P. Structural mechanism of plant aquaporin gating. Nature 2006; 439:688-94; PMID:16340961; http://dx.doi.org/10.1038/nature04316
4. Fuglsang AT, Visconti S, Drumm K, Jahn T, Stensballe A, Mattei B, Jensen ON, Aducci P, Palmgren MG. Binding of 14-3-3 protein to the plasma membrane H (+)-ATPase AHA2 involves the three C-terminal residues Tyr(946)-Thr-Val and requires phosphorylation of Thr(947). J Biol Chem 1999; 274:36774-80; PMID:10593986; http://dx.doi.org/10.1074/jbc.274.51.36774
5. Li W, Luan S, Schreiber SL, Assmann SM. Evidence for Protein Phosphatase 1 and 2A Regulation of K+ Channels in Two Types of Leaf Cells. Plant Physiol 1994; 106:963-70; PMID:7824661; http://dx.doi.org/10.1104/pp.106.3.963
6. Li J, Assmann SM. An Abscisic Acid-Activated and Calcium-Independent Protein Kinase from Guard Cells of Fava Bean. Plant Cell 1996; 8:2359-68; PMID:12239380; http://dx.doi.org/10.1105/tpc.8.12.2359
7. Geiger D, Maierhofer T, AL-Rasheid KAS, Scherzer S, Mumm P, Liese A, Ache P, Wellmann C, Marten I, Grill E, et al. Stomatal Closure by Fast Abscisic Acid Signaling Is Mediated by the Guard Cell Anion Channel SLAH3 and the Receptor RCAR1. Sci Signal 2011; 4(173):ra32; PMID:21586729; http://dx.doi.org/10.1126/scisignal.2001346
8. Geiger D, Scherzer S, Mumm P, Marten I, Ache P, Matschi S, Liese A, Wellmann C, Al-Rasheid KAS, Grill E, et al. Guard cell anion channel SLAC1 is regulated by CDPK protein kinases with distinct Ca^{2+} affinities. Proc Natl Acad Sci USA 2010; 107:8023-8; PMID:20385816; http://dx.doi.org/10.1073/pnas.0912030107
9. Geiger D, Scherzer S, Mumm P, Stange A, Marten I, Bauer H, Ache P, Matschi S, Liese A, Al-Rasheid KAS, et al. Activity of guard cell anion channel SLAC1 is controlled by drought-stress signaling kinase-phosphatase pair. Proc Natl Acad Sci USA 2009; 106:21425-30; PMID:19955405; http://dx.doi.org/10.1073/pnas.0912021106
10. Zourelidou M, Absmanner B, Weller B, Barbosa IC, Willige BC, Fastner A, Streit V, Port SA, Colcombet J, de la Fuente van Bentem S, et al. Auxin efflux by PIN-FORMED proteins is activated by two different protein kinases, D6 PROTEIN KINASE and PINOID. Elife 2014; 3; PMID:24948515
11. Prak S, Hem S, Boudet J, Viennois G, Sommerer N, Rossignol M, Maurel C, Santoni V. Multiple phosphorylations in the C-terminal tail of plant plasma membrane aquaporins. Mol Cell Proteomics 2008; 7:1019-30; PMID:18234664; http://dx.doi.org/10.1074/mcp.M700566-MCP200
12. Boursiac Y, Chen S, Luu DT, Sorieul M, van den Dries N, Maurel C. Early effects of salinity on water transport in Arabidopsis roots. Molecular and cellular features of aquaporin expression. Plant Physiol 2005; 139:790-805; PMID:16183846; http://dx.doi.org/10.1104/pp.105.065029
13. Liu KH, Tsay YF. Switching between the two action modes of the dual-affinity nitrate transporter CHL1 by phosphorylation. EMBO J 2003; 22:1005-13; PMID:12606566; http://dx.doi.org/10.1093/emboj/cdg118
14. Shoji T, Inai K, Yazaki Y, Sato Y, Takase H, Shitan N, Yazaki K, Goto Y, Toyooka K, Matsuoka K, et al. Multidrug and Toxic Compound Extrusion-Type Transporters Implicated in Vacuolar Sequestration of Nicotine in Tobacco Roots. Plant Physiol 2009; 149:708-18; PMID:19098091; http://dx.doi.org/10.1104/pp.108.132811
15. Morita M, Shitan N, Sawada K, Van Montagu MCE, Inze D, Rischer H, Goossens A, Oksman-Caldentey KM, Moriyama Y, Yazaki K. Vacuolar transport of nicotine is mediated by a multidrug and toxic compound extrusion (MATE) transporter in Nicotiana tabacum. Proc Natl Acad Sci USA 2009; 106:2447-52; PMID:19168636; http://dx.doi.org/10.1073/pnas.0812512106
16. Hildreth SB, Gehman EA, Yang HB, Lu RH, Ritesh KC, Harich KC, Yu S, Lin JS, Sandoe JL, Okumoto S, et al. Tobacco nicotine uptake permease (NUP1) affects alkaloid metabolism. Proc Natl Acad Sci USA 2011; 108:18179-84; PMID:22006310; http://dx.doi.org/10.1073/pnas.1108620108
17. Shitan N, Dalmas F, Dan K, Kato N, Ueda K, Sato F, Forestier C, Yazaki K. Characterization of Coptis japonica CjABCB2, an ATP-binding cassette protein involved in alkaloid transport. Phytochemistry 2012; 91:109-16; PMID:22410351; http://dx.doi.org/10.1016/j.phytochem.2012.02.012
18. Shitan N, Bazin I, Dan K, Obata K, Kigawa K, Ueda K, Sato F, Forestier C, Yazaki K. Involvement of CjMDR1, a plant multidrug-resistance-type ATP-binding cassette protein, in alkaloid transport in Coptis japonica. Proc Natl Acad Sci USA 2003; 100:751-6; PMID:12524452; http://dx.doi.org/10.1073/pnas.0134257100
19. Halkier BA, Gershenzon J. Biology and biochemistry of glucosinolates. Annu Rev Plant Biol 2006; 57:303-33; PMID:16669764; http://dx.doi.org/10.1146/annurev.arplant.57.032905.105228
20. Nour-Eldin HH, Andersen TG, Burow M, Madsen SR, Jorgensen ME, Olsen CE, Dreyer I, Hedrich R, Geiger D, Halkier BA. NRT/PTR transporters are essential for translocation of glucosinolate defence compounds to seeds. Nature 2012; 488:531-4; PMID:22864417; http://dx.doi.org/10.1038/nature11285
21. Leran S, Varala K, Boyer JC, Chiurazzi M, Crawford N, Daniel-Vedele F, David L, Dickstein R, Fernandez E, Forde B, et al. A unified nomenclature of NITRATE TRANSPORTER 1/PEPTIDE TRANSPORTER family members in plants. Trends Plant Sci 2013; 19 (1):5-9; PMID:24055139; http://dx.doi.org/10.1016/j.tplants.2013.08.008

22. Andersen TG, Nour-Eldin HH, Fuller VL, Olsen CE, Burow M, Halkier BA. Integration of Biosynthesis and Long-Distance Transport Establish Organ-Specific Glucosinolate Profiles in Vegetative Arabidopsis. Plant Cell 2013; 25(8):3133-45; PMID:23995084; http://dx.doi.org/10.1105/tpc.113.110890
23. Heazlewood JL, Durek P, Hummel J, Selbig J, Weckwerth W, Walther D, Schulze WX. PhosPhAt: a database of phosphorylation sites in Arabidopsis thaliana and a plant-specific phosphorylation site predictor. Nucleic Acids Res 2008; 36:D1015-21; PMID:17984086; http://dx.doi.org/10.1093/nar/gkm812
24. Benschop JJ, Mohammed S, O'Flaherty M, Heck AJR, Slijper M, Menke FLH. Quantitative phosphoproteomics of early elicitor signaling in Arabidopsis. Mol Cell Proteomics 2007; 6:1198-214; PMID:17317660; http://dx.doi.org/10.1074/mcp.M600429-MCP200
25. Chen Y, Hoehenwarter W, Weckwerth W. Comparative analysis of phytohormone-responsive phosphoproteins in Arabidopsis thaliana using TiO2-phosphopeptide enrichment and mass accuracy precursor alignment. Plant J 2010; 63:1-17; PMID:20374526; http://dx.doi.org/10.1111/j.1365-313X.2010.04261.x
26. Nuhse TS, Bottrill AR, Jones AME, Peck SC. Quantitative phosphoproteomic analysis of plasma membrane proteins reveals regulatory mechanisms of plant innate immune responses. Plant J 2007; 51:931-40; PMID:17651370; http://dx.doi.org/10.1111/j.1365-313X.2007.03192.x
27. Nuhse TS, Stensballe A, Jensen ON, Peck SC. Phosphoproteomics of the arabidopsis plasma membrane and a new phosphorylation site database. Plant Cell 2004; 16:2394-405; PMID:15308754; http://dx.doi.org/10.1105/tpc.104.023150
28. Biasini M, Bienert S, Waterhouse A, Arnold K, Studer G, Schmidt T, Kiefer F, Cassarino TG, Bertoni M, Bordoli L, et al. SWISS-MODEL: modelling protein tertiary and quaternary structure using evolutionary information. Nucleic Acids Res 2014; 42(Web Server issue):W252-8; PMID:24782522
29. Kelm S, Shi J, Deane CM. iMembrane: homology-based membrane-insertion of proteins. Bioinformatics 2009; 25:1086-8; PMID:19237449; http://dx.doi.org/10.1093/bioinformatics/btp102
30. Sun J, Bankston JR, Payandeh J, Hinds TR, Zagotta WN, Zheng N. Crystal structure of the plant dual-affinity nitrate transporter NRT1.1. Nature 2014; 507:73-7; PMID:24572362; http://dx.doi.org/10.1038/nature13074
31. Cuthbertson JM, Doyle DA, Sansom MSP. Transmembrane helix prediction: a comparative evaluation and analysis. Protein Engineering Design Selection 2005; 18:295-308; http://dx.doi.org/10.1093/protein/gzi032
32. Latz A, Becker D, Hekman M, Muller T, Beyhl D, Marten I, Eing C, Fischer A, Dunkel M, Bertl A, et al. TPK1, a Ca(2+)-regulated Arabidopsis vacuole two-pore K(+) channel is activated by 14-3-3 proteins. Plant J 2007; 52:449-59; PMID:17764516; http://dx.doi.org/10.1111/j.1365-313X.2007.03255.x
33. Latz A, Mehlmer N, Zapf S, Mueller TD, Wurzinger B, Pfister B, Csaszar E, Hedrich R, Teige M, Becker D. Salt stress triggers phosphorylation of the Arabidopsis vacuolar K+ channel TPK1 by calcium-dependent protein kinases (CDPKs). Mol Plant 2013; 6:1274-89; PMID:23253603; http://dx.doi.org/10.1093/mp/sss158
34. Parker JL, Newstead S. Molecular basis of nitrate uptake by the plant nitrate transporter NRT1.1. Nature 2014; 507:68-72; PMID:24572366; http://dx.doi.org/10.1038/nature13116
35. de Beer TA, Berka K, Thornton JM, Laskowski RA. PDBsum additions. Nucleic Acids Res 2014; 42:D292-6; PMID:24153109; http://dx.doi.org/10.1093/nar/gkt940
36. Geu-Flores F, Nour-Eldin HH, Nielsen MT, Halkier BA. USER fusion: a rapid and efficient method for simultaneous fusion and cloning of multiple PCR products. Nucleic Acids Res 2007; 35(7):e55; PMID:17389646; http://dx.doi.org/10.1093/nar/gkm106
37. Nour-Eldin HH, Hansen BG, Norholm MH, Jensen JK, Halkier BA. Advancing uracil-excision based cloning towards an ideal technique for cloning PCR fragments. Nucleic Acids Res 2006; 34:e122; PMID:17000637; http://dx.doi.org/10.1093/nar/gkl635